



THE UNIVERSITY *of* EDINBURGH

Edinburgh Research Explorer

The preterm cervix reveals a transcriptomic signature in the presence of premature pre-labor rupture of membranes

Citation for published version:

Makieva, S, Dubicke, A, Rinaldi, SF, Fransson, E, Ekman-Ordeberg, G & Norman, JE 2017, 'The preterm cervix reveals a transcriptomic signature in the presence of premature pre-labor rupture of membranes', *American Journal of Obstetrics & Gynecology (AJOG)*. <https://doi.org/10.1016/j.ajog.2017.02.009>

Digital Object Identifier (DOI):

[10.1016/j.ajog.2017.02.009](https://doi.org/10.1016/j.ajog.2017.02.009)

Link:

[Link to publication record in Edinburgh Research Explorer](#)

Document Version:

Peer reviewed version

Published In:

American Journal of Obstetrics & Gynecology (AJOG)

General rights

Copyright for the publications made accessible via the Edinburgh Research Explorer is retained by the author(s) and / or other copyright owners and it is a condition of accessing these publications that users recognise and abide by the legal requirements associated with these rights.

Take down policy

The University of Edinburgh has made every reasonable effort to ensure that Edinburgh Research Explorer content complies with UK legislation. If you believe that the public display of this file breaches copyright please contact openaccess@ed.ac.uk providing details, and we will remove access to the work immediately and investigate your claim.



Accepted Manuscript

The preterm cervix reveals a transcriptomic signature in the presence of premature pre-labor rupture of membranes

Sofia Makieva, PhD, Aurelija Dubicke, PhD, MD, Sara F. Rinaldi, PhD, Emma Fransson, PhD, Gunvor Ekman-Ordeberg, PhD, MD, Jane E. Norman, MD



PII: S0002-9378(17)30249-1

DOI: [10.1016/j.ajog.2017.02.009](https://doi.org/10.1016/j.ajog.2017.02.009)

Reference: YMOB 11529

To appear in: *American Journal of Obstetrics and Gynecology*

Received Date: 6 October 2016

Revised Date: 31 January 2017

Accepted Date: 6 February 2017

Please cite this article as: Makieva S, Dubicke A, Rinaldi SF, Fransson E, Ekman-Ordeberg G, Norman JE, The preterm cervix reveals a transcriptomic signature in the presence of premature pre-labor rupture of membranes, *American Journal of Obstetrics and Gynecology* (2017), doi: 10.1016/j.ajog.2017.02.009.

This is a PDF file of an unedited manuscript that has been accepted for publication. As a service to our customers we are providing this early version of the manuscript. The manuscript will undergo copyediting, typesetting, and review of the resulting proof before it is published in its final form. Please note that during the production process errors may be discovered which could affect the content, and all legal disclaimers that apply to the journal pertain.

Title: The preterm cervix reveals a transcriptomic signature in the presence of premature pre-labor rupture of membranes

Sofia Makieva, PhD ^{1*}, Aurelija Dubicke, PhD, MD ^{2*}, Sara F Rinaldi, PhD ¹, Emma Fransson, PhD ², Gunvor Ekman-Ordeberg, PhD, MD ², Jane E Norman, MD ¹
Edinburgh, UK
Stockholm, Sweden

¹Tommy's Centre for Maternal and Fetal Health, MRC Centre for Reproductive Health, EH16 4TJ Edinburgh UK

²Department of Women's and Children's Health, Karolinska Institute, 17176 Stockholm, Sweden

* Authors contributed equally

Disclosure statement: The authors report no conflict of interest.

Financial support: Supported by Tommy's Baby Charity funding to JEN and the Swedish Research Council funding to AD and GEO. The views expressed herein are of the authors and not an official position of the institutions or funders.

Corresponding author's details

Name: Sofia Makieva

Address: 47 Little France Crescent, QMRI, EH16 4TJ, Edinburgh, UK

Telephone: +44 0131 226613 Email: makievasofia@gmail.com

World counts

Abstract: 276

Main text: 3682

27 **Condensation:** The transcriptome of the human uterine cervix reveals a signature in the
28 presence of premature pre-labor rupture of fetal membranes.

29 **Short version of title:** The transcriptome of the preterm cervix

30

Abstract

Background: Premature Pre-labor Rupture of Fetal Membranes (PPROM) accounts for 30% of all premature births and is associated with detrimental long-term infant outcomes. Premature cervical remodeling, facilitated by matrix metalloproteinases (MMPs), may trigger rupture at the zone of the fetal membranes overlying the cervix. The similarities and differences underlying cervical remodeling in PPRM and spontaneous preterm labor with intact membranes (PTL) are unexplored. **Objectives:** We aimed a) to perform the first transcriptomic assessment of the preterm human cervix to identify differences between PPRM and PTL and b) to compare the enzymatic activities of MMP-2 and 9 between PPRM and PTL. **Study Design:** Cervical biopsies were collected following PTL (n=6) and PPRM (n=5). Biopsies were also collected from reference groups at term labor (TL; n=12) or term not labor (TNL; n=5). The Illumina HT-12 v4.0 BeadChips microarray was utilized and a novel network graph approach determined the specificity of changes between PPRM and PTL. qRT-PCR and Western blotting confirmed the microarray findings. Immunofluorescence was employed for localization studies and gelatin zymography to assess MMP activity. **Results:** PRAM1, FGD3 and CEACAM3 were significantly higher whereas NDRG2 lower in the PPRM cervix when compared to the cervix in PTL, TL and TNL. PRAM1 and CEACAM3 were localized to immune cells at the cervical stroma and NDRG2 and FGD3 were localized to cervical myofibroblasts. The activity of MMP-9 was higher (1.22 ± 4.403 fold, $p < 0.05$) in the cervix in PPRM compared to PTL. **Conclusions:** We identified four novel proteins with a potential role in the regulation of cervical remodeling leading to PPRM. Our findings contribute to the studies dissecting the mechanisms underlying PPRM and inspire further investigations towards the development of PPRM therapeutics.

55 **Keywords:** cervix, metalloproteinases, microarray, preterm labor, premature rupture of fetal

56 membranes

57

Introduction

Preterm birth (PTB), defined as birth before 37 completed weeks of gestation, remains the major cause of neonatal morbidity and mortality affecting approximately 1 million pregnancies each year ¹. PTBs are predominantly spontaneous in nature and only 25% are iatrogenic ². Spontaneous PTBs (sPTBs) can be the outcome of spontaneous preterm labor with intact membranes (PTL; 45% of all sPTBs) or preterm pre-labor rupture of membranes (PPROM; 30% of all sPTBs) ². Although PTL is likely to follow PPROM, PTL and PPROM can present as separate entities due to differences in their initiating triggers and the underlying pathways leading to premature cervical remodeling ³.

The pathophysiology of PPROM has been poorly explored. It is believed that the tensile strength of the fetal membranes can be reduced by premature cervical dilation, which can expose the weakest zone of the fetal membranes to vaginal microorganisms and reduce the underlying tissue support ⁴. Indeed, microbial invasion of the amniotic cavity (MIAC) is present in approximately 30–40% of patients with PPROM ⁵. It is noteworthy that premature cervical remodeling in the absence of infection can also result in unscheduled rupture of fetal membranes. What triggers these cervical changes in the absence of infection and how these fine-tune the timing of rupture is currently unknown. Genetic factors have been proposed to predispose women to PPROM and a recent systematic review ⁶ reported that specific polymorphisms were associated with PPROM in blood ⁷⁻⁹, amnion ^{10, 11} and buccal swabs ^{12, 13}. From these a main regulation axis for PPROM was proposed consisting of pathways regulating hematologic/coagulation function disorder, local inflammation, collagen metabolism and matrix degradation. Notably, pregnant women with Ehlers-Danlos syndrome, an inherited connective tissue disorder resulting from mutations in genes responsible for collagen structure and/or synthesis, have increased risk for PPROM ^{14, 15}. A proteomic study

of the human placenta additionally demonstrated an association of PPROM with alterations in structural/cytoskeletal components of cells and impaired regulation of energy metabolism and oxidative stress¹⁶.

In light of the detrimental impact of PPROM on long-term infant outcomes¹⁷, the early and accurate prediction of the condition could allow for timely intervention in order to improve perinatal outcomes and reduce obstetric complications, such as chorioamnionitis, neonatal sepsis or cord prolapse. Assessment of the cervical length and detection of biomarkers in biological fluids of symptomatic women serves to confirm suspected cases of PTL and MIAC-associated PPROM^{18, 19} but a test which predicts PPROM before it occurs is yet to be developed.

Understanding the differences and similarities in the underlying pathologies associated with PPROM and PTL will allow new avenues for research and treatment. Herein we hypothesized that different cervical remodeling events facilitate PPROM and PTL. We set out to explore whether these different events would manifest as a PPROM-specific gene signature. To our knowledge this is the first genome-wide approach study utilizing human cervical biopsies to study PPROM and PTL as individual groups.

Materials and Methods

Human cervical biopsies

Cervical biopsies were collected at the Karolinska Hospital during 2006-2008 following the informed consent and approval of the local Ethics Committee. Biopsies were taken directly (within 30 minutes) after vaginal delivery or caesarean section (CS) transvaginally (at 12

o'clock position) from anterior cervical lip with scissors and tweezers. A total of 28 women were recruited: 6 undergoing spontaneous preterm labor (PTL), 5 with preterm premature rupture of membranes (PPROM) followed by labor, 12 undergoing normal term labor (TL) and 5 who delivered at term prior to the onset of labor (TNL). Preterm delivery was defined as delivery before the 37th week of gestation. Women in the PTL, PPRM and TL groups were in active labor and demonstrated a ripe cervix, with dilatation of more than 4 cm. All except two of these subjects delivered vaginally. One woman in the PTL group delivered by emergency CS due to breech presentation and one in the TL group due to protracted labor. PPRM was defined as a rupture of membranes at least one hour before onset of contractions². TNL samples were obtained from women undergoing planned CS with unripe cervix. None of the subjects had clinical signs of infection or chorioamnionitis nor suffered from pre-eclampsia, diabetes or other systemic disease. There were no significant differences between the groups of pregnant women with respect to maternal age, parity or previous preterm births. For clinical data of the recruited subjects consult Table 1 Supplemental.

Sample processing

The samples were processed for RNA and protein extraction or fixed as detailed in Supplemental Material and Methods 1.

Illumina HT-12 v4.0 BeadChip expression microarray

A total of 23 samples were QC analyzed using the arrayQualityMetrics package in Bioconductor²¹ and no outliers were identified. The samples were split randomly over the Illumina HT-12 v4.0 BeadChips to minimize any effect of inter-chip variability. The chips were imaged using a BeadArray Reader and raw data were obtained with Illumina

BeadStudio software. Raw and processed data are available at www.ebi.ac.uk/arrayexpress/ under accession number E-MTAB-5354.

Microarray analysis

Fios Genomics Ltd (Bioquarter, Edinburgh, UK) performed the statistical analysis of the array as described in Supplemental Material and Methods 2.

Network graph analysis

Normalized expression data generated by microarray analysis were further filtered to include only the genes up- or down-regulated genes ($p < 0.05$, fold-change = any) in at least at 1 out of 6 comparisons in order to eliminate the noise created by genes with conserved expression. That final dataset was used as an input for Biolayout Express3D (BLE) analysis software to create sample-sample and a gene-gene network graphs as previously described^{22, 23} and further detailed in Supplemental Material and Methods 3.

QRT-PCR

Quantitative RT-PCR (singleplex) was performed to validate the differences identified in the microarray and BLE analysis. The original samples used in the microarray were used for the validation, in addition to 5 new TL samples. Details about the assay are available in Supplemental Material and Methods 4.

Western blotting and Immunofluorescence

Western blotting and immunofluorescence were used to quantify and localize PRAM1, FGD3, CEACAM3 and NDRG2 proteins in the cervix as described in Supplemental Material and Methods 5.

Gelatin Zymography

A total of 20 µg protein was loaded onto precast 10% Novex® gelatin-containing gels (Thermo Scientific, Wilmington, DE, USA) and separated by electrophoresis. Subsequently, the gels were incubated with Novex® renaturing and Novex® developing buffer according to manufacturers' protocol (Thermo Scientific, Wilmington, DE, USA). Staining was then performed using the Novex® SimplyBlue SafeStain solution until the sites of membrane degradation by MMP-2 or MMP-9 manifested as bands on the zymographs. Zymography bands were quantified using Adobe Photoshop's CS6 histogram function.

Statistics

Graphpad Prism 6 (La Jolla, CA 92037 USA) was used for the statistical analysis of the qRT-PCR, Western blotting and Zymography data. For qRT-PCR, the thresholds for the gene of interest (GOI) and actin-β (ACTB) were set in the linear phase of the exponential region of the amplification curves. The cycle number at which the PCR signal crossed a set threshold was used to determine relative gene expression. The average comparative cycle threshold (Ct) values for the GOI and ACTB were used to calculate ΔC_t and the number was normalized ($\Delta\Delta C_t$) to the PPRM group. $\Delta\Delta C_t$ values were used for statistical analysis and data were plotted as fold change ($2^{(-\Delta\Delta C_t)}$). For Western blotting, the intensity of band fluorescence was analyzed and the readout value for statistical analysis was the raw ratio of fluorescence intensity value of protein of interest (POI) and α-Tubulin (POI: α-Tubulin). For zymography, the readout for statistical analysis was the raw pixel number for each band. All data were initially analyzed for normal distribution using the Kolmogorov-Smirnov test. Western blotting (raw fluorescence ratio) and qRT-PCR ($\Delta\Delta C_t$) data were analyzed with one-way ANOVA Dunnett's test to compare each group to PPRM. Zymography data (raw pixel

number) were analyzed with one-way ANOVA Tukey's test. Significance was set at $p < 0.05$. Error bars denote standard error of the mean (SEM).

Results

Microarray identified gene expression differences between PPRM and PTL.

A sample-sample network graph followed by Markov Cluster Algorithm (MCL α =19.3) analysis was generated from normalized microarray data (**Figure 1A, B, C**) to understand the relationship between samples at a finer level. The proximity of samples implied similarity in genetic signature (**Figure 1A**) and MCL analysis of the samples identified four clusters (**Figure B**). When nodes were coloured according to their group status (**Figure 1C**) it became evident that all 5 TNL samples belonged to MCL cluster i, where they shared cluster membership with 2 PTL samples. Additionally, MCL cluster ii contained 5 out of 7 TL samples, which shared cluster membership with 4 PTL samples. 3 out of 5 PPRM samples formed their own cluster (MCL cluster iii) and 1 PPRM sample clustered with 2 TL samples to form MCL cluster iv. One PPRM sample did not cluster with others, suggesting it did not genetically identify with other samples. Importantly, PPRM and PTL samples did not share cluster membership and 60% of PPRM samples clustered together suggesting a distinct genetic signature specific to the PPRM pathology. Indeed, a strict cut-off revealed that 44 genes were differentially expressed between the PPRM and PTL groups (**Figure 1D**) out of which 32 were significantly up-regulated and 12 down-regulated (**Figure 2A**). A list of these genes is shown in **Table 1**. A heatmap analysis (**Figure 2B**) allowed for visual identification of the genes with a conserved PPRM-specific high or low expression across all PPRM samples when compared to all other samples (i.e. *FGD3*, *LILRA5*, *NDRG2*, *PRAMI*, *CD300LF*, *CEACAM3*, *PPDPF*, *RNA28S*). Significantly changed genes in the

PPROM-PTL comparison were analyzed for enrichment of Kyoto Encyclopedia of Genes and Genomes (KEGG) pathway membership (**Table 2**) and Gene Ontology (GO) terms (**Table 3**). ‘Osteoclast differentiation’ was the only overexpressed KEGG pathway in the PPROM group, when compared to PTL, with 5 significant genes up-regulated and 19 GO terms associated with immunity were enriched.

Pathological gene signature associated with PPROM.

The normalized microarray data for the 30 up- and 9 down- regulated genes in the PPROM-PTL comparison were used as input to generate two gene-gene network graphs, where each node represented a gene. MCL analysis (MCLi =1.3) was performed to give an unbiased assessment of how the up- regulated (**Figure 3A**) and down-regulated genes (**Figure 3B**) clustered. We identified 6 MCL clusters for the up- and 3 for the down-regulated genes (**Figure 3C**) and the average (mean) gene expression profile for each cluster was examined to detect a PPROM-specific signature (**Figure 3D-L**). As with the heatmap, we identified the clusters with a high or low averaged expression of genes conserved across all PPROM samples. Analysis of MCL cluster 4 (**Figure 3G**) and 5 (**Figure 3H**) revealed that the averaged expression of genes in MCL cluster 4 (*STK4*, *CEACAM3*, *FGD3*) and MCL cluster 5 (*PRAMI*, *MYO1F*) was higher in the PPROM samples when compared with PTL, TL and TNL samples. MCL cluster interpretation relied on visual observation and no statistics were applied at that stage. From the down-regulated MCL clusters, MCL 8 showed a low averaged expression for *NDRG2* and *ACOT13* in the PPROM samples (**Figure 3K**). None of the other clusters suggested trends worthy of further investigation. From the pool of 7 genes identified (*STK4*, *CEACAM3*, *FGD3*, *PRAMI*, *MYO1F*, *NDRG2* and *ACOT13*), statistical significance between PPROM compared to PTL, TL and TNL was reached for *CEACAM3* (**Figure 4A**), *PRAMI* (**Figure 4D**), *FGD3* (**Figure 4G**), and *NDRG2* (**Figure 4J**) as reported by traditional

microarray analysis performed by Fios Genomics, which was further validated with qRT-PCR and Western blotting. Specifically, the mRNA concentration of CEACAM3 (**Figure 4B**) was 2.17 ± 0.17 fold lower in the PTL group, 1.79 ± 0.12 fold lower in the TL group and 3.97 ± 0.03 fold lower in the TNL group when compared to PPRM. These values for PRAM1 (**Figure 4E**) were 2.55 ± 0.17 fold for PTL, 1.85 ± 0.35 fold for TL and 4.8 ± 0.1 fold for TNL. The concentration of FGD3 mRNA (**Figure 4H**) was also 3.34 ± 0.11 fold lower in PTL, 3.29 ± 0.08 fold lower in TL and 2.7 ± 0.18 fold lower in TNL when compared to PPRM. In contrast, the mRNA of NDRG2 was in lower concentration in the PPRM cervix when compared to PTL (-4.16 ± 0.57), TL (-3.62 ± 0.63) and TNL (-4.0 ± 0.42) groups (**Figure 4K**). These changes were confirmed in the protein level. CEACAM3 (**Figure 4C**) and FGD3 (**Figure 4I**) were significantly higher in the PPRM group when compared to the other groups. CEACAM3 was 2.57 ± 0.06 fold lower in the PTL cervix, 2.65 ± 0.07 fold lower in the TL cervix and 2.77 ± 0.07 fold lower in the TNL cervix. These values for FGD3 were 1.88 ± 0.09 for PTL, 2.02 ± 0.18 for TL and 2.58 ± 0.24 for TNL. PRAM1 (**Figure 4F**) was significantly higher in PPRM compared to PTL (2.97 ± 0.15) and TL (3.5 ± 0.08) but not TNL. NDRG2 (**Figure 4L**) protein was significantly lower in the PPRM group when compared to PTL (-6.78 ± 0.5) and TL (7.0 ± 0.54) but not TNL group.

PPROM-specific markers were localized to immune cells and vascular myofibroblasts.

We explored the localization of PRAM1, CEACAM3, FGD3 and NDRG2 within the cervical tissue. Although the literature suggests that PRAM1 is predominantly expressed in granulocytes it did not co-localize with the established granulocyte membrane marker CEACAM3 (**Figure 5D**). Instead, PRAM1 was localized to the cytoplasm of a subset of immune CD45 positive cells (**Figure 5H**) resident in the cervical stroma (**Figure 5C, F, I, M**). Notably, all PRAM1 positive cells stained for CD45, suggesting that these are immune

cells. We confirmed that PRAM1 positive cells were neither macrophages (**Figure 5K**) nor neutrophils (**Figure 5O**). Positive, albeit marginal, NDRG2 staining was evident in the nuclei of the endocervical epithelial cells (**Figure 6C**), which were positive for pan-cytokeratin (**Figure 6B**). Strong NDRG2 staining (**Figure 6G**) was detected in the cytoplasm of endocervical glands (**Figure 6F**) and myofibroblasts surrounding blood vessels in the cervical stroma (**Figure 6D**). A double staining with Von Willebrand factor (vWF), a marker expressed in the endothelial cells of the vasculature, confirmed the blood vessel status (**Figure 6J**). FDG3 was also expressed in the cytoplasm of myofibroblasts (**Figure 6P**) surrounding vWF positive blood vessels (**Figure 6N**). We found that NDRG2 and FGD3 shared the same localization within myofibroblasts (**Figure 6T**).

GO terms for PRAM1, CEACAM3, FGD3 and NDRG2.

All GO enriched terms for the PPROM-specific markers can be found in **Table 4**.

The activity of Matrix Metalloproteinase 9 (MMP-9) was higher in the PPROM cervix.

Gelatin zymography revealed that the activity of MMP-9 (**Figure 7A**), but not MMP-2 (**Figure 7B**), was significantly higher in the PPROM cervix. Specifically, the activity of MMP-9 was higher 1.22 ± 4.403 fold in PPROM when compared to PTL ($p < 0.05$), 1.25 ± 4.328 fold compared to TL ($p < 0.05$) and 1.57 ± 6.600 fold compared to TNL ($p < 0.001$) (**Figure 7A**).

Comment

This is the first transcriptomic study of the preterm human cervix, which examined PTL and PPROM as two separate pathologies and compared gene expression in the two groups. According to a recent systematic review, only 4% of all transcriptomic studies in term and

preterm human pregnancies have utilized cervical tissue and, strikingly, none of these has examined PPROM individually²⁴. Several genetic polymorphisms associated with PPROM have been identified in the placenta, membranes and maternal/fetal blood [reviewed in⁶] and smaller-scale studies also demonstrated the presence of PPROM-associated inflammatory markers in the amniotic fluid^{25, 26}, fetal membranes²⁷⁻²⁹ and maternal serum³⁰. All these studies combined with recent proteomic¹⁶ and epigenetic³¹ reports of a PPROM signature in the placenta and maternal blood have established the hypothesis that PPROM and PTL may have distinct underlying pathologies. It remained to be deduced whether a PPROM signature would be detected in the cervix. We hypothesized that the cervix might initiate rupture of the fetal membranes at their contact site through PPROM-specific cervical remodeling events. Our findings support this hypothesis and demonstrate that PPROM is associated with expression of key proteins, which may facilitate the organization of the cervical extracellular matrix (ECM) and indirectly accelerate membranes rupture.

The GO terms for the overexpressed genes in PPROM, when compared to PTL (Table 3), were predominantly related to immunity, for example ‘immune system processes’, ‘immunity mediated by myeloid leukocytes’ and ‘immunity mediated by neutrophils’. This is perhaps not surprising because physiological cervical remodeling is accompanied by infiltration of leukocyte subpopulations and neutrophils, which work to achieve the rigidity of the cervix³².³³. In line with our findings, a study in the mouse cervix proved that the overarching mechanism underlying cervical remodeling-associated immune cell influx is similar in term and preterm parturition and only marginal differences occur whereby the mediators and effector cells involved may differ³⁴. Our findings provide the first evidence to suggest that the immunity modulators employed to mediate cervical remodeling may be additionally different between the preterm subgroups PPROM and PTL. Immune modulators stimulate

immune and other cells in the cervical stroma to produce cytokines and MMPs to degrade the ECM as part of the remodeling process^{35, 4}. MMP-2 and MMP-9 are gelatinases both capable of degrading collagens type I and III, the main constituents of the cervical ECM³⁶. MMP-2 and MMP-9 concentration is reportedly elevated in the amniotic fluid of PPROM pregnancies²⁵. Both MMP-2 and MMP-9 are produced by human cervical fibroblasts²⁰ and MMP-9 by vascular fibroblasts^{37, 38} and neutrophil granulocytes³⁹⁻⁴¹. To contribute to the notion that the facilitators of ECM degradation may differ between PPROM and PTL or TL in the cervix, we performed an assay to assess MMP-2 and MMP-9 activity. Indeed, the activity of MMP-9 was increased solely in PPROM.

Out of the 44 differentially expressed genes between the PPROM and PTL groups identified with traditional array analysis, our network graph analysis followed by validation, brought forward 4 key proteins that were over- or under- expressed only in the PPROM cervix. Although these proteins are novel to the parturition field, there is some evidence to support that they might be involved in the activation of a pathological cascade, which delivers a “rupture” signal to the weakest zone of fetal membranes overlying the cervix. Specifically, NDRG2 may be switched off in cervical myofibroblasts to promote the production of MMP-9 and accelerate a PPROM-specific remodeling process. Down-regulation of NDRG2 has been previously associated with an increase in the gelatinolytic activities of MMP-2 and MMP-9⁴² in adenocarcinomic human alveolar basal epithelial cell line and more reports have shown direct inhibition of MMP-9 activity by NDRG2⁴³⁻⁴⁵. In support of this hypothesis, cathepsin D (CTSD), which is also down-regulated in PPROM compared to PTL (Table 1) and shares GO terms with NDRG2 (Table 4), is additionally a negative regulator of MMP-2 and MMP-9 in endometriotic lesions⁴⁶. CEACAM3, a membrane granulocyte protein involved in neutrophil activation^{47, 48}, and FGD3 may also work together towards enhancement of MMP-

9 activity in PPROM. It is not unlikely that aberrant infiltrating neutrophil-granulocytes overexpress CEACAM3 to promote their activation and stimulate MMP-9 secretion. In support of this notion, genes that share GO terms with *CEACAM3* (Table 4) have also been associated with MMP actions. For example, the osteoclast-associated markers *OSCAR* and *SIRPA* and *TREM-1* have all been implicated in MMP-9-mediated responses⁴⁹⁻⁵². CEACAM3 shares cluster membership with FGD3 (Figure 3C), suggesting similar regulation in gene expression, which itself may imply similar functions. FGD3 may control MMP-9 activity in the PPROM cervix by promoting filopodia formation on the plasma membranes of myofibroblasts⁵³. It is well established that proteins of the same family with FGD3 organize such formations on plasma membranes to release MMPs and in turn induce degradation of the surrounding stroma^{54, 55}. Remarkably, blockade of filopodia formation by flavonoids has been shown to decrease the release of MMP-2 in cancer⁵⁶. Electron microscopy studies could help investigate filopodial formations on cells in PPROM. PRAM1, which shared GO terms with FGD3 (Table 4), is thought to be predominantly expressed in granulocyte-neutrophils where it acts as an adaptor protein critical for select integrin functions⁵⁷. Integrins are transmembrane receptors that bridge cell-ECM interactions and activate MMPs⁵⁸. A proteolytic role for integrins has been described in the initiation of labor, whereby they regulate release of MMP-9 in human fetal membranes⁵⁹. Although we did not detect PRAM1 in elastase positive neutrophils or in CEACAM3 positive granulocytes (Figure 5), the likelihood of PRAM1 regulating integrin functions in the cytoplasm of an alternative immune cell population in the cervix deserves addressing.

Employing a genome-wide approach has identified key genes associated with PPROM, and provided an insight into a potential mechanism regulating physiological cervical remodeling. Analysis of the two top clusters of the up-regulated genes in PPROM (Figure 3D, E)

demonstrated that the genes within these clusters were overexpressed both in PPRM and, surprisingly, in TL. The first overexpressed cluster contained various genes involved in bone marrow-derived cell migration (*ARHGAP9*, *FGR*, *NFE2*) and *SLC43A2*, the gene coding an essential transporter of Branched Chain Amino Acids (BCAAs). We propose a new mechanism to contribute to cervical remodeling in TL and PPRM, whereby the increase of BCAAs in the cervix triggers the recruitment of bone marrow-derived cells in order to stimulate MMP-induced degradation. Consistent with our hypothesis, MMP-2 and MMP-9 increase in response to exogenous BCAAs in the hippocampus of rats⁶⁰ and bone marrow-derived cells have been also shown to secrete MMPs⁶¹⁻⁶³. A similar mechanism for cervical remodeling in TL and PPRM involving bone marrow recruited cells can be further evidenced by KEGG analysis, where ‘Osteoclast differentiation’ pathway is enriched not only in PPRM-PTL comparison (Table 2) but also in TL-PTL (Table 3 Supplemental). Osteoclasts are bone marrow-derived cells traditionally involved in the degradation of bone matrix⁶⁴ and have been described to secrete MMP-2 and MMP-9^{62, 63}. Further work is required to prove whether bone marrow-derived osteoclasts or osteoclast-like cells mediate MMPs-induced degradation of ECM as part of physiological cervical remodeling cascade. It is noteworthy that only 16 genes were differentially expressed between PPRM and TL, in contrast to 1285 genes in the TNL-TL comparison. The notion that PPRM and TL might share some similar pathways for cervical remodeling was additionally supported by the sample-sample network graph (Figure 1C). In that graph PPRM and TL samples belonged to the same ‘loose’ local structure whereas the TNL samples belong to a separate ‘tight’ structure.

Our study could benefit from a larger sample size but human cervical biopsies are extremely hard to obtain especially in relation to preterm delivery, which explains why so few studies

are conducted on the human preterm cervix. Moreover, the biopsies were collected postpartum and thus postpartum repair mechanism might be reflected in our results. However, it is not practically and ethically possible to obtain cervical biopsies during vaginal delivery and the material used in our study was collected within 30 minutes after delivery. Animal research, for example CRISPR experiments could be useful in future studies, to identify the phenotype associated with knock out or knock in of the genes we suggest are important.

In summary, we have, for the first time identified a gene expression signature involved with PPROM. It is tempting to hypothesize that the PPROM-specific proteins identified herein act as contributors in a pathway whereby MMP-9 facilitates ECM degradation in the cervix to signal a 'rupture' message to the overlying membranes. Our work supports the growing body of evidence suggesting that premature labor is a multifactorial disorder with different pathways involved for PPROM and PTL.

397 **Acknowledgments**

398 The authors thank Mr Ronnie Grant for illustration services.

399

References

- [1] Blencowe H, Cousens S, Oestergaard MZ, Chou D, Moller AB, Narwal R, Adler A, Vera Garcia C, Rohde S, Say L, Lawn JE: National, regional, and worldwide estimates of preterm birth rates in the year 2010 with time trends since 1990 for selected countries: a systematic analysis and implications. *Lancet* 2012, 379:2162-72.
- [2] Goldenberg RL, Culhane JF, Iams JD, Romero R: Epidemiology and causes of preterm birth. *Lancet* 2008, 371:75-84.
- [3] Srinivas SK, Macones GA: Preterm premature rupture of the fetal membranes: current concepts. *Minerva Ginecol* 2005, 57:389-96.
- [4] Strauss JF, 3rd: Extracellular matrix dynamics and fetal membrane rupture. *Reprod Sci* 2013, 20:140-53.
- [5] Bopegamage S, Kacerovsky M, Tambor V, Musilova I, Sarmirova S, Snelders E, de Jong AS, Vari SG, Melchers WJ, Galama JM: Preterm prelabor rupture of membranes (PPROM) is not associated with presence of viral genomes in the amniotic fluid. *J Clin Virol* 2013, 58:559-63.
- [6] Capece A, Vasieva O, Meher S, Alfirovic Z, Alfirovic A: Pathway analysis of genetic factors associated with spontaneous preterm birth and pre-labor preterm rupture of membranes. *PLoS One* 2014, 9:e108578.
- [7] Roberts AK, Monzon-Bordonaba F, Van Deerlin PG, Holder J, Macones GA, Morgan MA, Strauss JF, 3rd, Parry S: Association of polymorphism within the promoter of the tumor

420 necrosis factor alpha gene with increased risk of preterm premature rupture of the fetal
421 membranes. *Am J Obstet Gynecol* 1999, 180:1297-302.

422 [8] Romero R, Friel LA, Velez Edwards DR, Kusanovic JP, Hassan SS, Mazaki-Tovi S,
423 Vaisbuch E, Kim CJ, Erez O, Chaiworapongsa T, Pearce BD, Bartlett J, Salisbury BA, Anant
424 MK, Vovis GF, Lee MS, Gomez R, Behnke E, Oyarzun E, Tromp G, Williams SM, Menon
425 R: A genetic association study of maternal and fetal candidate genes that predispose to
426 preterm prelabor rupture of membranes (PROM). *Am J Obstet Gynecol* 2010, 203:361 e1-
427 e30.

428 [9] Valdez-Velazquez LL, Quintero-Ramos A, Perez SA, Mendoza-Carrera F, Montoya-
429 Fuentes H, Rivas F, Jr., Olivares N, Celis A, Vazquez OF, Rivas F: Genetic polymorphisms
430 of the renin-angiotensin system in preterm delivery and premature rupture of membranes. *J*
431 *Renin Angiotensin Aldosterone Syst* 2007, 8:160-8.

432 [10] Fujimoto T, Parry S, Urbanek M, Sammel M, Macones G, Kuivaniemi H, Romero R,
433 Strauss JF, 3rd: A single nucleotide polymorphism in the matrix metalloproteinase-1 (MMP-
434 1) promoter influences amnion cell MMP-1 expression and risk for preterm premature
435 rupture of the fetal membranes. *J Biol Chem* 2002, 277:6296-302.

436 [11] Wang H, Parry S, Macones G, Sammel MD, Kuivaniemi H, Tromp G, Argyropoulos G,
437 Halder I, Shriver MD, Romero R, Strauss JF, 3rd: A functional SNP in the promoter of the
438 SERPINH1 gene increases risk of preterm premature rupture of membranes in African
439 Americans. *Proc Natl Acad Sci U S A* 2006, 103:13463-7.

440 [12] Kalish RB, Nguyen DP, Vardhana S, Gupta M, Perni SC, Witkin SS: A single
441 nucleotide A>G polymorphism at position -670 in the Fas gene promoter: relationship to

442 preterm premature rupture of fetal membranes in multifetal pregnancies. *Am J Obstet*
443 *Gynecol* 2005, 192:208-12.

444 [13] Kalish RB, Vardhana S, Normand NJ, Gupta M, Witkin SS: Association of a maternal
445 CD14 -159 gene polymorphism with preterm premature rupture of membranes and
446 spontaneous preterm birth in multi-fetal pregnancies. *Journal of reproductive immunology*
447 2006, 70:109-17.

448 [14] De Vos M, Nuytinck L, Verellen C, De Paepe A: Preterm premature rupture of
449 membranes in a patient with the hypermobility type of the Ehlers-Danlos syndrome. A case
450 report. *Fetal Diagn Ther* 1999, 14:244-7.

451 [15] Hermanns-Le T, Pierard G, Quatresooz P: Ehlers-Danlos-like dermal abnormalities in
452 women with recurrent preterm premature rupture of fetal membranes. *Am J Dermatopathol*
453 2005, 27:407-10.

454 [16] Chang A, Zhang Z, Zhang L, Gao Y, Zhang L, Jia L, Cui S, Wang P: Proteomic analysis
455 of preterm premature rupture of membranes in placental tissue. *Arch Gynecol Obstet* 2013,
456 288:775-84.

457 [17] Clark EA, Varner M: Impact of preterm PROM and its complications on long-term
458 infant outcomes. *Clin Obstet Gynecol* 2011, 54:358-69.

459 [18] Tambor V, Kacerovsky M, Andrys C, Musilova I, Hornychova H, Pliskova L, Link M,
460 Stulik J, Lenco J: Amniotic fluid cathelicidin in PPRM pregnancies: from proteomic
461 discovery to assessing its potential in inflammatory complications diagnosis. *PLoS One* 2012,
462 7:e41164.

- [19] Vuadens F, Benay C, Crettaz D, Gallot D, Sapin V, Schneider P, Bienvenut WV, Lemery D, Quadroni M, Dastugue B, Tissot JD: Identification of biologic markers of the premature rupture of fetal membranes: proteomic approach. *Proteomics* 2003, 3:1521-5.
- [20] Dubicke A, Akerud A, Sennstrom M, Hamad RR, Bystrom B, Malmstrom A, Ekman-Ordeberg G: Different secretion patterns of matrix metalloproteinases and IL-8 and effect of corticotropin-releasing hormone in preterm and term cervical fibroblasts. *Mol Hum Reprod* 2008, 14:641-7.
- [21] Kauffmann A, Huber W: Microarray data quality control improves the detection of differentially expressed genes. *Genomics* 2010, 95:138-42.
- [22] Sharp GC, Hutchinson JL, Hibbert N, Freeman TC, Saunders PT, Norman JE: Transcription Analysis of the Myometrium of Laboring and Non-Laboring Women. *PLoS One* 2016, 11:e0155413.
- [23] Theocharidis A, van Dongen S, Enright AJ, Freeman TC: Network visualization and analysis of gene expression data using BioLayout Express(3D). *Nat Protoc* 2009, 4:1535-50.
- [24] Eidem HR, Ackerman WEt, McGary KL, Abbot P, Rokas A: Gestational tissue transcriptomics in term and preterm human pregnancies: a systematic review and meta-analysis. *BMC Med Genomics* 2015, 8:27.
- [25] Fortunato SJ, Menon R, Lombardi SJ: MMP/TIMP imbalance in amniotic fluid during PROM: an indirect support for endogenous pathway to membrane rupture. *J Perinat Med* 1999, 27:362-8.

- [26] Romero R, Chaiworapongsa T, Alpay Savasan Z, Xu Y, Hussein Y, Dong Z, Kusanovic JP, Kim CJ, Hassan SS: Damage-associated molecular patterns (DAMPs) in preterm labor with intact membranes and preterm PROM: a study of the alarmin HMGB1. *J Matern Fetal Neonatal Med* 2011, 24:1444-55.
- [27] Fortunato SJ, Menon R, Bryant C, Lombardi SJ: Programmed cell death (apoptosis) as a possible pathway to metalloproteinase activation and fetal membrane degradation in premature rupture of membranes. *Am J Obstet Gynecol* 2000, 182:1468-76.
- [28] Menon R, Lombardi SJ, Fortunato SJ: IL-18, a product of choriodecidual cells, increases during premature rupture of membranes but fails to turn on the Fas-FasL-mediated apoptosis pathway. *J Assist Reprod Genet* 2001, 18:276-84.
- [29] Canzonieri BJ, Feng L, Grotegut CA, Bentley RC, Heine RP, Murtha AP: The chorion layer of fetal membranes is prematurely destroyed in women with preterm premature rupture of the membranes. *Reprod Sci* 2013, 20:1246-54.
- [30] Hajek Z, Germanova A, Koucky M, Zima T, Kopecky P, Vitkova M, Parizek A, Kalousova M: Detection of feto-maternal infection/inflammation by the soluble receptor for advanced glycation end products (sRAGE): results of a pilot study. *J Perinat Med* 2008, 36:399-404.
- [31] Luo X, Shi Q, Gu Y, Pan J, Hua M, Liu M, Dong Z, Zhang M, Wang L, Gu Y, Zhong J, Zhao X, Jenkins EC, Brown WT, Zhong N: LncRNA pathway involved in premature preterm rupture of membrane (PPROM): an epigenomic approach to study the pathogenesis of reproductive disorders. *PLoS One* 2013, 8:e79897.

- 504 [32] Sakamoto Y, Moran P, Bulmer JN, Searle RF, Robson SC: Macrophages and not
505 granulocytes are involved in cervical ripening. *Journal of reproductive immunology* 2005,
506 66:161-73.
- 507 [33] Kelly RW: Inflammatory mediators and cervical ripening. *Journal of reproductive*
508 *immunology* 2002, 57:217-24.
- 509 [34] Gonzalez JM, Dong Z, Romero R, Girardi G: Cervical remodeling/ripening at term and
510 preterm delivery: the same mechanism initiated by different mediators and different effector
511 cells. *PLoS One* 2011, 6:e26877.
- 512 [35] Read CP, Word RA, Ruscheinsky MA, Timmons BC, Mahendroo MS: Cervical
513 remodeling during pregnancy and parturition: molecular characterization of the softening
514 phase in mice. *Reproduction* 2007, 134:327-40.
- 515 [36] Gonzalez JM, Romero R, Girardi G: Comparison of the mechanisms responsible for
516 cervical remodeling in preterm and term labor. *Journal of reproductive immunology* 2013,
517 97:112-9.
- 518 [37] Ma J, Ma SY, Ding CH: Curcumin reduces cardiac fibrosis by inhibiting myofibroblast
519 differentiation and decreasing transforming growth factor beta1 and matrix metalloproteinase
520 9 / tissue inhibitor of metalloproteinase 1. *Chin J Integr Med* 2016.
- 521 [38] Tomita K, Takashina M, Mizuno N, Sakata K, Hattori K, Imura J, Ohashi W, Hattori Y:
522 Cardiac fibroblasts: contributory role in septic cardiac dysfunction. *The Journal of surgical*
523 *research* 2015, 193:874-87.

- 524 [39] Deryugina EI, Zajac E, Juncker-Jensen A, Kupriyanova TA, Welter L, Quigley JP:
525 Tissue-infiltrating neutrophils constitute the major in vivo source of angiogenesis-inducing
526 MMP-9 in the tumor microenvironment. *Neoplasia* 2014, 16:771-88.
- 527 [40] Bausch D, Pausch T, Krauss T, Hopt UT, Fernandez-del-Castillo C, Warshaw AL,
528 Thayer SP, Keck T: Neutrophil granulocyte derived MMP-9 is a VEGF independent
529 functional component of the angiogenic switch in pancreatic ductal adenocarcinoma.
530 *Angiogenesis* 2011, 14:235-43.
- 531 [41] Mente J, Petrovic J, Gehrig H, Rampf S, Michel A, Schurz A, Pfefferle T, Saure D,
532 Erber R: A Prospective Clinical Pilot Study on the Level of Matrix Metalloproteinase-9 in
533 Dental Pulpal Blood as a Marker for the State of Inflammation in the Pulp Tissue. *J Endod*
534 2016, 42:190-7.
- 535 [42] Faraji SN, Mojtahedi Z, Ghalamfarsa G, Takhshid MA: N-myc downstream regulated
536 gene 2 overexpression reduces matrix metalloproteinase-2 and -9 activities and cell invasion
537 of A549 lung cancer cell line in vitro. *Iran J Basic Med Sci* 2015, 18:773-9.
- 538 [43] Lee DG, Lee SH, Kim JS, Park J, Cho YL, Kim KS, Jo DY, Song IC, Kim N, Yun HJ,
539 Park YJ, Lee SJ, Lee HG, Bae KH, Lee SC, Shim S, Kim YM, Kwon YG, Kim JM, Lee HJ,
540 Min JK: Loss of NDRG2 promotes epithelial-mesenchymal transition of gallbladder
541 carcinoma cells through MMP-19-mediated Slug expression. *J Hepatol* 2015, 63:1429-39.
- 542 [44] Ma Q, Li HF, Jin S, Dou XC, Zhang YF, Zhang LX, Du ZR: [Inhibitory effects of
543 17beta-estradiol on spontaneous and activated contraction of rat uterus smooth muscle].
544 *Zhongguo ying yong sheng li xue za zhi = Zhongguo yingyong shenglixue zazhi = Chinese*
545 *journal of applied physiology* 2013, 29:305-9.

- 546 [45] Shon SK, Kim A, Kim JY, Kim KI, Yang Y, Lim JS: Bone morphogenetic protein-4
547 induced by NDRG2 expression inhibits MMP-9 activity in breast cancer cells. *Biochem*
548 *Biophys Res Commun* 2009, 385:198-203.
- 549 [46] Protopapas A, Markaki S, Mitsis T, Milingos D, Athanasiou S, Haidopoulos D,
550 Loutradis D, Antsaklis A: Immunohistochemical expression of matrix metalloproteinases,
551 their tissue inhibitors, and cathepsin-D in ovarian endometriosis: correlation with severity of
552 disease. *Fertil Steril* 2010, 94:2470-2.
- 553 [47] Sarantis H, Gray-Owen SD: Defining the roles of human carcinoembryonic antigen-
554 related cellular adhesion molecules during neutrophil responses to *Neisseria gonorrhoeae*.
555 *Infect Immun* 2012, 80:345-58.
- 556 [48] Zhang S, Tu YT, Cai HH, Ding HH, Li Q, He YX, Liu XX, Wang X, Hu F, Chen T,
557 Chen HX: Opacity proteins of *neisseria gonorrhoeae* in lipooligosaccharide mutants lost
558 ability to interact with neutrophil-restricted CEACAM3 (CD66d). *J Huazhong Univ Sci*
559 *Technol Med Sci* 2016, 36:344-9.
- 560 [49] Gomez-Pina V, Martinez E, Fernandez-Ruiz I, Del Fresno C, Soares-Schanoski A,
561 Jurado T, Siliceo M, Toledano V, Fernandez-Palomares R, Garcia-Rio F, Arnalich F, Biswas
562 SK, Lopez-Collazo E: Role of MMPs in orchestrating inflammatory response in human
563 monocytes via a TREM-1-PI3K-NF-kappaB pathway. *J Leukoc Biol* 2012, 91:933-45.
- 564 [50] Ruhul Amin AR, Uddin Biswas MH, Senga T, Feng GS, Kannagi R, Agarwal ML,
565 Hamaguchi M: A role for SHPS-1/SIRPalpha in Concanavalin A-dependent production of
566 MMP-9. *Genes Cells* 2007, 12:1023-33.

- 567 [51] Junrui P, Bingyun L, Yanhui G, Xu J, Darko GM, Dianjun S: Relationship between
568 fluoride exposure and osteoclast markers during RANKL-induced osteoclast differentiation.
569 *Environ Toxicol Pharmacol* 2016, 46:241-5.
- 570 [52] Rao VH, Rai V, Stoupa S, Subramanian S, Agrawal DK: Data on TREM-1 activation
571 destabilizing carotid plaques. *Data Brief* 2016, 8:230-4.
- 572 [53] Nakanishi H, Takai Y: Frabin and other related Cdc42-specific guanine nucleotide
573 exchange factors couple the actin cytoskeleton with the plasma membrane. *Journal of cellular*
574 *and molecular medicine* 2008, 12:1169-76.
- 575 [54] He P, Wu W, Yang K, Tan D, Tang M, Liu H, Wu T, Zhang S, Wang H: Rho Guanine
576 Nucleotide Exchange Factor 5 Increases Lung Cancer Cell Tumorigenesis via MMP-2 and
577 Cyclin D1 Upregulation. *Mol Cancer Ther* 2015, 14:1671-9.
- 578 [55] Murphy DA, Courtneidge SA: The 'ins' and 'outs' of podosomes and invadopodia:
579 characteristics, formation and function. *Nat Rev Mol Cell Biol* 2011, 12:413-26.
- 580 [56] Santos BL, Oliveira MN, Coelho PL, Pitanga BP, da Silva AB, Adelita T, Silva VD,
581 Costa Mde F, El-Bacha RS, Tardy M, Chneiweiss H, Junier MP, Moura-Neto V, Costa SL:
582 Flavonoids suppress human glioblastoma cell growth by inhibiting cell metabolism,
583 migration, and by regulating extracellular matrix proteins and metalloproteinases expression.
584 *Chem Biol Interact* 2015, 242:123-38.
- 585 [57] Clemens RA, Newbrough SA, Chung EY, Gheith S, Singer AL, Koretzky GA, Peterson
586 EJ: PRAM-1 is required for optimal integrin-dependent neutrophil function. *Mol Cell Biol*
587 2004, 24:10923-32.

- 588 [58] Sato T, Sakai T, Noguchi Y, Takita M, Hirakawa S, Ito A: Tumor-stromal cell contact
589 promotes invasion of human uterine cervical carcinoma cells by augmenting the expression
590 and activation of stromal matrix metalloproteinases. *Gynecol Oncol* 2004, 92:47-56.
- 591 [59] Ahmed N, Riley C, Oliva K, Barker G, Quinn MA, Rice GE: Expression and
592 localization of α v β 6 integrin in extraplacental fetal membranes: possible role in human
593 parturition. *Mol Hum Reprod* 2004, 10:173-9.
- 594 [60] Scaini G, Morais MO, Galant LS, Vuolo F, Dall'Igna DM, Pasquali MA, Ramos VM,
595 Gelain DP, Moreira JC, Schuck PF, Ferreira GC, Soriano FG, Dal-Pizzol F, Streck EL:
596 Coadministration of branched-chain amino acids and lipopolysaccharide causes matrix
597 metalloproteinase activation and blood-brain barrier breakdown. *Mol Neurobiol* 2014,
598 50:358-67.
- 599 [61] Chaudhary AK, Chaudhary S, Ghosh K, Shanmukaiah C, Nadkarni AH: Secretion and
600 Expression of Matrix Metalloproteinase-2 and 9 from Bone Marrow Mononuclear Cells in
601 Myelodysplastic Syndrome and Acute Myeloid Leukemia. *Asian Pac J Cancer Prev* 2016,
602 17:1519-29.
- 603 [62] Liu B, Cui J, Sun J, Li J, Han X, Guo J, Yi M, Amizuka N, Xu X, Li M:
604 Immunolocalization of MMP9 and MMP2 in osteolytic metastasis originating from MDA-
605 MB-231 human breast cancer cells. *Mol Med Rep* 2016, 14:1099-106.
- 606 [63] Ohshiba T, Miyaura C, Inada M, Ito A: Role of RANKL-induced osteoclast formation
607 and MMP-dependent matrix degradation in bone destruction by breast cancer metastasis. *Br J*
608 *Cancer* 2003, 88:1318-26.

609 [64] Boyle WJ, Simonet WS, Lacey DL: Osteoclast differentiation and activation. Nature
610 2003, 423:337-42.

611

612

613 **Tables**614 **Table 1:** List of up and down-regulated genes

| | Symbol | FC | Adj.P.Val |
|------|----------|---------|-----------|
| Up | PRAM1 | 2.094 | 1.36E-04 |
| | SIRPA | 2.101 | 1.36E-04 |
| | CEACAM3 | 2.412 | 2.92E-04 |
| | CD300LF | 2.232 | 1.82E-03 |
| | LILRA2 | 2.598 | 2.42E-03 |
| | FGD3 | 2.735 | 2.42E-03 |
| | OSCAR | 2.168 | 2.65E-03 |
| | TREM1 | 3.826 | 2.65E-03 |
| | OSCAR | 2.351 | 2.65E-03 |
| | STK4 | 2.023 | 2.65E-03 |
| | NUDT11 | 2.233 | 3.09E-03 |
| | LILRA6 | 2.522 | 3.09E-03 |
| | MAMLD1 | 2.821 | 3.23E-03 |
| | ASGR1 | 2.063 | 3.42E-03 |
| | MYO1F | 2.004 | 3.77E-03 |
| | MMP25 | 3.117 | 3.77E-03 |
| | TMEM71 | 2.269 | 4.96E-03 |
| | CSF3R | 4.164 | 4.96E-03 |
| | FGR | 3.036 | 6.00E-03 |
| | PRDM8 | 2.577 | 6.00E-03 |
| | NLRP12 | 2.211 | 6.00E-03 |
| | FGR | 2.668 | 6.00E-03 |
| | NFE2 | 4.23 | 6.29E-03 |
| | FKBP1A | 2.25 | 6.38E-03 |
| | SLC43A2 | 2.067 | 7.72E-03 |
| | CLEC5A | 2.374 | 7.87E-03 |
| | LILRA5 | 2.781 | 7.87E-03 |
| | ARHGAP9 | 2.107 | 8.72E-03 |
| | GK | 2.837 | 9.61E-03 |
| | CYTH4 | 2.437 | 9.66E-03 |
| Down | NDRG2 | -3.551 | 7.52E-04 |
| | PPDPF | -5.093 | 3.09E-03 |
| | RNU4ATAC | -3.67 | 3.23E-03 |
| | PKM | -3.278 | 6.00E-03 |
| | ACOT13 | -2.171 | 6.00E-03 |
| | CTSD | -2.031 | 6.38E-03 |
| | RETSAT | -2.565 | 7.00E-03 |
| | RNA28S5 | -11.005 | 7.87E-03 |
| | RNA28S5 | -6.788 | 8.72E-03 |

Footnote Table 1: Adj.P.Val: at the adjusted p-value < 0.01, FC: fold change >= 2

618 **Table 2:** KEGG pathway enrichment analysis of the up and down-regulated genes that
 619 mapped to significant features at adjusted p<0.05.

| | Name of KEGG pathway | Pvalue | Genes | No. Sig. Genes | % Sig. Genes |
|----|----------------------------|----------|--------------------------------------|----------------|--------------|
| Up | Osteoclast differentiation | 4.34E-06 | LILRA2, LILRA5, LILRA6, OSCAR, SIRPA | 5 | 4.1 |

| | | | | | |
|------|-------------------------------------|----------|--------|---|-----|
| Down | Pyruvate metabolism | 2.03E-02 | PKM | 1 | 2.8 |
| | Retinol metabolism | 2.03E-02 | RETSAT | 1 | 2.8 |
| | Type II diabetes mellitus | 2.08E-02 | PKM | 1 | 2.7 |
| | Glycolysis / Gluconeogenesis | 3.20E-02 | PKM | 1 | 1.8 |
| | Central carbon metabolism in cancer | 3.42E-02 | PKM | 1 | 1.6 |
| | Glucagon signaling pathway | 4.74E-02 | PKM | 1 | 1.2 |

Table 3: GO term enrichment analysis of the up and down-regulated genes that mapped to significant features at adjusted $p < 0.001$

| | Ontology | Name | Pvalue | Genes | No. Sig. Genes | % Sig. Genes |
|------|----------|---|----------|---|----------------|--------------|
| Up | BP | immune system process | 3.44E-06 | CD300LF, CLEC5A, CSF3R, FGR, FKBP1A, LILRA2, LILRA5, LILRA6, MYO1F, NLRP12, PRAM1, SIRPA, STK4, TREM1 | 14 | 0.7 |
| | BP | defense response | 3.38E-04 | CLEC5A, CSF3R, FGR, LILRA2, LILRA5, MMP25, MYO1F, NLRP12, TREM1 | 9 | 0.8 |
| | BP | myeloid leukocyte mediated immunity | 3.73E-06 | FGR, MYO1F, PRAM1, TREM1 | 4 | 7.4 |
| | BP | cytokine secretion | 6.77E-05 | CLEC5A, FGR, NLRP12, TREM1 | 4 | 3.6 |
| | BP | protein secretion | 4.86E-04 | CLEC5A, FGR, NLRP12, TREM1 | 4 | 2.1 |
| | BP | leukocyte mediated immunity | 6.62E-04 | FGR, MYO1F, PRAM1, TREM1 | 4 | 2 |
| | BP | neutrophil mediated immunity | 1.07E-05 | MYO1F, PRAM1, TREM1 | 3 | 13.6 |
| | BP | leukocyte degranulation | 8.96E-05 | FGR, MYO1F, PRAM1 | 3 | 6.8 |
| | BP | regulated secretory pathway | 1.75E-04 | FGR, MYO1F, PRAM1 | 3 | 5.5 |
| | BP | myeloid cell activation involved in immune response | 1.75E-04 | FGR, MYO1F, PRAM1 | 3 | 5.5 |
| | BP | positive regulation of cytokine secretion | 2.50E-04 | CLEC5A, FGR, NLRP12 | 3 | 4.8 |
| | BP | positive regulation of protein secretion | 7.97E-04 | CLEC5A, FGR, NLRP12 | 3 | 3.3 |
| | BP | regulation of cytokine secretion | 8.75E-04 | CLEC5A, FGR, NLRP12 | 3 | 3.2 |
| | BP | neutrophil degranulation | 1.72E-04 | MYO1F, PRAM1 | 2 | 20 |
| | BP | neutrophil activation involved in immune response | 2.52E-04 | MYO1F, PRAM1 | 2 | 16.7 |
| | BP | neutrophil activation | 8.72E-04 | MYO1F, PRAM1 | 2 | 9.1 |
| | BP | regulation of myeloid leukocyte mediated immunity | 9.54E-04 | FGR, PRAM1 | 2 | 8.7 |
| | BP | regulation of leukocyte degranulation | 9.54E-04 | FGR, PRAM1 | 2 | 8.7 |
| | BP | regulation of regulated secretory pathway | 9.54E-04 | FGR, PRAM1 | 2 | 8.7 |
| Down | MF | pyruvate kinase activity | 8.24E-04 | PKM | 1 | 50 |
| | MF | all-trans-retinol 13,14-reductase activity | 4.12E-04 | RETSAT | 1 | 100 |

Footnote Table 3: BP: Biological Process, MF: Molecular Function

Table 4: Report of the GO terms containing the features PRAM1, FGD3, CEACAM3 and NDRG2 amongst other genes that mapped to significant features at adjusted $p < 0.01$.

| | Gene | Ontology | Name | Pvalue | Genes | No. Sig. Genes | % Sig. Genes |
|------|---------|----------|---|----------|--|----------------|--------------|
| Up | PRAM1 | BP | response to stimulus | 1.12E-02 | ARHGAP9, ASGR1, CLEC5A, CSF3R, CYTH4, FGD3, FGR, FKBP1A, LILRA2, LILRA5, MMP25, MYO1F, NFE2, NLRP12, PRAM1, SIRPA, STK4, TREM1 | 18 | 0.3 |
| | | BP | immune system process | 3.44E-06 | CD300LF, CLEC5A, CSF3R, FGR, FKBP1A, LILRA2, LILRA5, LILRA6, MYO1F, NLRP12, PRAM1, SIRPA, STK4, TREM1 | 14 | 0.7 |
| | | BP | cell communication | 2.44E-02 | ARHGAP9, ASGR1, CLEC5A, CSF3R, CYTH4, FGD3, FGR, FKBP1A, LILRA2, NFE2, NLRP12, PRAM1, STK4, TREM1 | 14 | 0.3 |
| | | BP | immune response | 6.07E-03 | CLEC5A, FGR, FKBP1A, LILRA5, MYO1F, PRAM1, TREM1 | 7 | 0.6 |
| | | BP | secretion by cell | 1.64E-03 | CLEC5A, FGR, MYO1F, NLRP12, PRAM1, TREM1 | 6 | 0.9 |
| | | BP | secretion | 3.04E-03 | CLEC5A, FGR, MYO1F, NLRP12, PRAM1, TREM1 | 6 | 0.8 |
| | | BP | myeloid leukocyte mediated immunity | 3.73E-06 | FGR, MYO1F, PRAM1, TREM1 | 4 | 7.4 |
| | | BP | leukocyte mediated immunity | 6.62E-04 | FGR, MYO1F, PRAM1, TREM1 | 4 | 2 |
| | | BP | regulation of secretion | 1.01E-02 | CLEC5A, FGR, NLRP12, PRAM1 | 4 | 0.9 |
| | | BP | immune effector process | 1.74E-02 | FGR, MYO1F, PRAM1, TREM1 | 4 | 0.8 |
| | | BP | leukocyte activation | 2.33E-02 | FGR, FKBP1A, MYO1F, PRAM1 | 4 | 0.7 |
| | | BP | regulation of immune response | 4.03E-02 | FGR, FKBP1A, MYO1F, PRAM1 | 4 | 0.6 |
| | | BP | neutrophil mediated immunity | 1.07E-05 | MYO1F, PRAM1, TREM1 | 3 | 13.6 |
| | | BP | leukocyte degranulation | 8.96E-05 | FGR, MYO1F, PRAM1 | 3 | 6.8 |
| | | BP | regulated secretory pathway | 1.75E-04 | FGR, MYO1F, PRAM1 | 3 | 5.5 |
| | | BP | myeloid cell activation involved in immune response | 1.75E-04 | FGR, MYO1F, PRAM1 | 3 | 5.5 |
| | | BP | myeloid leukocyte activation | 2.02E-03 | FGR, MYO1F, PRAM1 | 3 | 2.4 |
| | | BP | leukocyte activation involved in immune response | 2.95E-03 | FGR, MYO1F, PRAM1 | 3 | 2.1 |
| | | BP | cell activation involved in immune response | 2.95E-03 | FGR, MYO1F, PRAM1 | 3 | 2.1 |
| | | BP | exocytosis | 1.66E-02 | FGR, MYO1F, PRAM1 | 3 | 1.1 |
| | | MF | lipid binding | 4.65E-02 | ARHGAP9, CYTH4, PRAM1 | 3 | 0.7 |
| | | BP | neutrophil degranulation | 1.72E-04 | MYO1F, PRAM1 | 2 | 20 |
| | | BP | neutrophil activation involved in immune response | 2.52E-04 | MYO1F, PRAM1 | 2 | 16.7 |
| | | BP | neutrophil activation | 8.72E-04 | MYO1F, PRAM1 | 2 | 9.1 |
| | | BP | regulation of myeloid leukocyte mediated immunity | 9.54E-04 | FGR, PRAM1 | 2 | 8.7 |
| | | BP | regulation of leukocyte degranulation | 9.54E-04 | FGR, PRAM1 | 2 | 8.7 |
| | | BP | regulation of regulated secretory pathway | 9.54E-04 | FGR, PRAM1 | 2 | 8.7 |
| | | BP | granulocyte activation | 1.04E-03 | MYO1F, PRAM1 | 2 | 8.3 |
| | | BP | integrin-mediated signaling pathway | 1.16E-02 | FGR, PRAM1 | 2 | 2.4 |
| | | BP | regulation of exocytosis | 1.30E-02 | FGR, PRAM1 | 2 | 2.3 |
| | | BP | regulation of leukocyte mediated immunity | 1.80E-02 | FGR, PRAM1 | 2 | 1.9 |
| | | BP | regulation of neutrophil degranulation | 8.01E-03 | PRAM1 | 1 | 25 |
| | | BP | regulation of neutrophil activation | 1.00E-02 | PRAM1 | 1 | 20 |
| | FGD3 | BP | response to stimulus | 1.12E-02 | ARHGAP9, ASGR1, CLEC5A, CSF3R, CYTH4, FGD3, FGR, FKBP1A, LILRA2, LILRA5, MMP25, MYO1F, NFE2, NLRP12, PRAM1, SIRPA, STK4, TREM1 | 18 | 0.3 |
| | | BP | cell communication | 2.44E-02 | ARHGAP9, ASGR1, CLEC5A, CSF3R, CYTH4, FGD3, FGR, FKBP1A, LILRA2, NFE2, NLRP12, PRAM1, STK4, TREM1 | 14 | 0.3 |
| | | BP | intracellular signal transduction | 2.54E-02 | ARHGAP9, CYTH4, FGD3, FGR, FKBP1A, NLRP12, STK4, TREM1 | 8 | 0.4 |
| | | BP | positive regulation of molecular function | 1.45E-02 | ARHGAP9, CYTH4, FGD3, FGR, FKBP1A, NLRP12, STK4 | 7 | 0.5 |
| | | BP | regulation of phosphate metabolic process | 2.58E-02 | ARHGAP9, CYTH4, FGD3, FGR, FKBP1A, NLRP12, STK4 | 7 | 0.5 |
| | | BP | regulation of phosphorus metabolic process | 2.69E-02 | ARHGAP9, CYTH4, FGD3, FGR, FKBP1A, NLRP12, STK4 | 7 | 0.5 |
| | | BP | positive regulation of catalytic activity | 2.40E-02 | ARHGAP9, CYTH4, FGD3, FGR, NLRP12, STK4 | 6 | 0.5 |
| | | BP | regulation of intracellular signal transduction | 3.39E-02 | ARHGAP9, CYTH4, FGD3, FGR, FKBP1A, NLRP12 | 6 | 0.5 |
| | | BP | regulation of hydrolase activity | 4.74E-02 | ARHGAP9, CYTH4, FGD3, FKBP1A, NLRP12 | 5 | 0.5 |
| | | BP | regulation of small GTPase mediated signal transduction | 4.97E-02 | ARHGAP9, CYTH4, FGD3 | 3 | 0.7 |
| | | BP | positive regulation of GTPase activity | 4.71E-02 | ARHGAP9, CYTH4, FGD3 | 3 | 0.7 |
| | | BP | regulation of cell shape | 1.73E-02 | FGD3, FGR | 2 | 2 |
| | | CC | ruffle | 3.15E-02 | FGD3, FGR | 2 | 1.5 |
| | | MF | guanyl-nucleotide exchange factor activity | 3.71E-02 | CYTH4, FGD3 | 2 | 1.2 |
| | | BP | regulation of Cdc42 GTPase activity | 3.94E-02 | FGD3 | 1 | 5 |
| | | BP | regulation of Cdc42 protein signal transduction | 4.52E-02 | FGD3 | 1 | 4.3 |
| | CEACAM3 | CC | membrane part | 6.82E-03 | ASGR1, CD300LF, CEACAM3, CLEC5A, CSF3R, FGR, FKBP1A, LILRA2, LILRA5, LILRA6, MMP25, OSCAR, SIRPA, SLC43A2, TMEM71, TREM1 | 16 | 0.4 |
| | | CC | integral component of membrane | 6.91E-03 | ASGR1, CD300LF, CEACAM3, CLEC5A, CSF3R, LILRA2, LILRA5, LILRA6, MMP25, OSCAR, SIRPA, SLC43A2, TMEM71, TREM1 | 14 | 0.4 |
| | | CC | intrinsic component of membrane | 8.61E-03 | ASGR1, CD300LF, CEACAM3, CLEC5A, CSF3R, LILRA2, LILRA5, LILRA6, MMP25, OSCAR, SIRPA, SLC43A2, TMEM71, TREM1 | 14 | 0.4 |
| Down | NDRG2 | CC | extracellular vesicular exosome | 4.17E-03 | ACOT13, CTSD, NDRG2, PKM | 4 | 0.2 |
| | | CC | extracellular membrane-bounded organelle | 4.17E-03 | ACOT13, CTSD, NDRG2, PKM | 4 | 0.2 |
| | | CC | extracellular organelle | 4.17E-03 | ACOT13, CTSD, NDRG2, PKM | 4 | 0.2 |
| | | CC | membrane-bounded vesicle | 9.41E-03 | ACOT13, CTSD, NDRG2, PKM | 4 | 0.1 |
| | | BP | regulation of platelet-derived growth factor production | 1.45E-03 | NDRG2 | 1 | 33.3 |
| | | BP | platelet-derived growth factor production | 1.45E-03 | NDRG2 | 1 | 33.3 |

Footnote Table 4: BP: Biological Process, MF: Molecular Function, CC: Cellular Component

Figure legends

Figure 1: Sample-sample network graph of all samples used for the microarray and the comparisons performed between the groups. A 2D representation of sample clustering in a 3D graph. Each node represents a different sample and edges are coloured to reflect the Pearson correlation that they represent. Red and blue edges denote high correlation and low correlation respectively. The same graph is coloured by **A.** no cluster ($r=0.91$), **B.** unbiased MCL cluster number (MCL 19.3) **C.** group status. **D:** Table shows all the comparisons performed between groups and the number of significant array features at adjusted p-value < 0.01 and fold change ≥ 2 . TL = Term Labor (n=7), TNL = Term Non-Labor (n=5), PTL=Preterm Labor (n=6), PPRM=Preterm Premature Rupture of Membranes (n=5).

Figure 2: PPRM vs PTL comparison. **A.** Volcano plot and **B.** heatmap showing the 30 features significant up-regulated (red dots) and 9 down-regulated (blue dots) at adjusted p-value < 0.01 and fold change ≥ 2 in the PPRM group compared to PTL group. A heatmap shows how genes and samples cluster based on similar expression levels. The bars at the top indicate the sample group (dark green = TNL, dark blue = PTL, light green = TL, light blue = PPRM). Normalized expression values are indicated on a color scale with red denoting high expression and blue low expression.

Figure 3: Probe-probe network cluster analysis. Probe-probe network graph of the up-regulated (**A**) and down-regulated (**B**) genes in the PPRM-PTL comparison. Each node represents a gene and nodes are coloured according to membership of different MCL (MCL $i = 1, 3$) clusters. **C:** The genes belonging to each cluster are shown in the MCL gene clusters table. The Pareto scaled graphs show the mean expression profiles of MCL clusters 1 (**D**), 2

(E), 3 (F), 4 (G), 5 (H), 6 (I), 7 (J), 8 (K), 9 (L) across all samples (n=23), including the samples in the TL and TNL groups. Samples are plotted on the x-axes. Genes with similar expression pattern across all samples are members of the same cluster. Each bar represents the average expression of all genes that cluster together in that sample. The error bar for each sample denotes the SD extrapolated from the expression of all cluster genes in that sample. PPRM n=5, PTL n=6, TL n=7, TNL n=5.

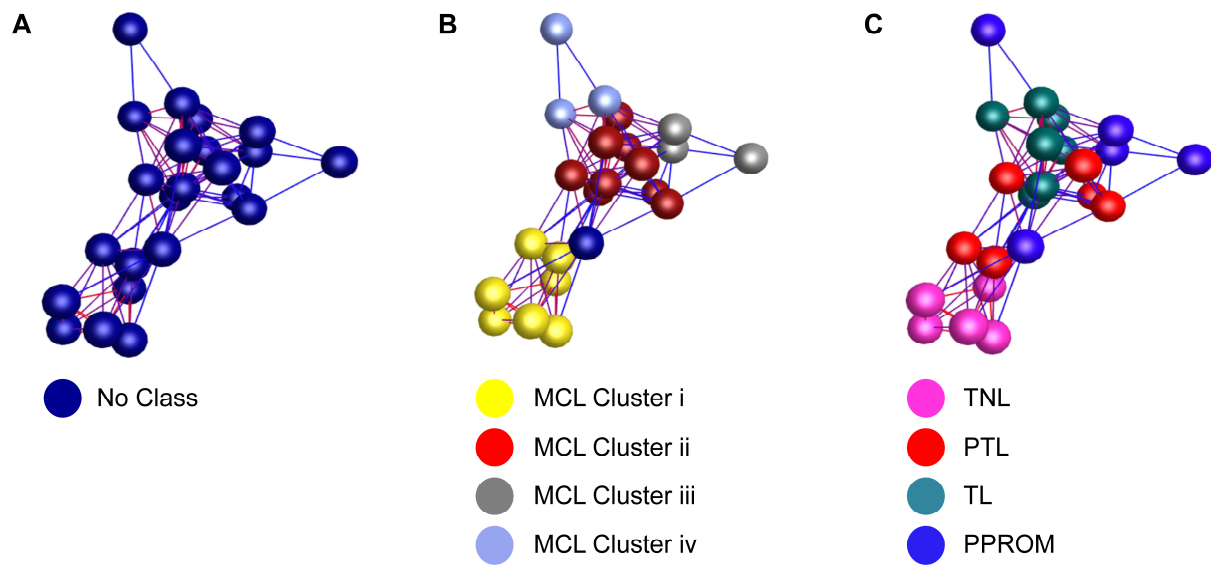
Figure 4: Validation of microarray analysis. A, D, G, J: Tables show the fold-changes (FC) and adjusted p values (Adj.P.Val) across all comparisons for the 4 selected genes CEACAM3, PRAM1, FGD3 and NDRG2 as reported by FIOS genomics statistical analysis. qRT-PCR validated that *CEACAM3* (B), *PRAM1* (E) and *FGD3* (H) were up-regulated, and *NDRG2* (K) down-regulated in the PPRM group when compared to all other groups. Data analyzed using one-way ANOVA Dunnett's test. qRT-PCR samples: PPRM n=5, PTL n=6, TL n=12, TNL n=5. Western blotting analysis confirmed that CEACAM3 (C) and FGD3 (I) were in higher concentration in the PPRM cervix compared to all other groups. PRAM1 (F) and NDRG2 (L) changes were also significant between PPRM and PTL/TL but not in TNL. Data analyzed using one-way ANOVA Dunnett's test. Western blotting samples: PPRM n=4, PTL n=4, TL n=4, TNL n=4. Error bars denote \pm SEM. *p<0.05, **p <0.01, ***p<0.001.

Figure 5: Localization of PRAM1 and CEACAM3 in the PPRM human cervix. PRAM1 and CEACAM3 positive cells were identified at the cervical stroma. PRAM1 was localized to the cytoplasm and CEACAM3 to the membrane of cells. CEACAM3 (B) and PRAM1 (C) did not co-localize (D). Double staining for PRAM1 (F) and CD45 (G) identified double positive population (H). PRAM1 cells (I), did not co-localize (K) with the

macrophage marker CD68 (**J**). PRAM1 cells (**M**) did not co-localize (**O**) with neutrophil Elastase (**N**). All scale bars 50 μ m. Images representative of n=4.

Figure 6: Localization of FGD3 and NDRG2 in the human cervix. Marginal NDRG2 staining (**C**) was detected to the nuclei of endocervical epithelial cells stained positive for AE1/AE3 (**D**). **D**: NDRG2 staining was evidently stronger in cells surrounding blood vessels (indicated with asterisks). A co-staining for vWF (**J**; an endothelial cell marker) and NDRG2 (**K**) confirmed that NDRG2 is localized to the cytoplasm of myofibroblasts surrounding blood vessels (**L**). NDRG2 was also localized to the cytoplasm of endocervical glandular cells (**G**) as was evident by co-localization (**H**) with AE1/AE3 (**F**). FGD3 was expressed solely in the cytoplasm of myofibroblasts (**O**) and co-localized with NDRG2 (**T**). Scale bars 50 μ m/ 100 μ m as shown in each picture. Images representative of n=4. **A-L**: PTL cervix, **M-P**: PPROM cervix, **Q-T**: TL cervix. vWF: Von Willebrand factor, AE1/AE3: Pan Cytokeratin.

Figure 7: MMP-2 and MMP-9 activity in the human cervix. Gelatin zymography was performed on protein extracted from the cervix of women with PPROM (n=4), PTL (n=4), TL (n=4) and TNL (n=4). **A**: The activity of MMP-9 (82 kDa) was significantly higher in the PPROM cervix when compared to the other groups (*p=0.05, ***p=0.001 comparison). **B**: The activity of MMP-2 was similar in PPROM, PTL and TL but significantly lower in TNL when compared to the other groups (****p<0.0001). Data analyzed using one-way ANOVA Tukey's test.



D

| Comparison | Significant genes |
|------------|-------------------|
| TL-TNL | 1285 |
| TL-PTL | 19 |
| TL-PPROM | 16 |
| TNL-PTL | 93 |
| TNL-PPROM | 886 |
| PPROM-PTL | 44 |

